Carbohydrate Polymers 229 (2020) 115551

Contents lists available at ScienceDirect

Carbohydrate Polymers

journal homepage: www.elsevier.com/locate/carbpol

Promoted chondrogenesis of hMCSs with controlled release of TGF-β3 via microfluidics synthesized alginate nanogels

Zahra Mahmoudi[a], Javad Mohammadnejad[a,*], Sajad Razavi Bazaz[b], Ali Abouei Mehrizi[a], Masoud Saidijam[c], Rassoul Dinarvand[d], Majid Ebrahimi Warkiani[b,e], Masoud Soleimani[f,*]

[a] Department of Life Science Engineering, Faculty of New Sciences and Technologies, University of Tehran, Tehran, Iran
[b] School of Biomedical Engineering, University of Technology Sydney, Sydney, NSW 2007, Australia
[c] Research Center for Molecular Medicine, Hamadan University of Medical Sciences, Hamadan, Iran
[d] Nanotechnology Research Centre, Novel Drug Delivery Department, Faculty of Pharmacy, Tehran University of Medical Science, Tehran, Iran
[e] Institute of Molecular Medicine, Sechenov University, Moscow, 119991, Russia
[f] Tissue engineering and Hematology Department, Faculty of Medical Sciences, Tarbiat Modares University, Tehran, Iran

ARTICLE INFO

Keywords:
Microfluidics
Computational fluid dynamics (CFD)
Alginate nanogels
Growth factor delivery
Chondrogenesis

ABSTRACT

The field of cartilage tissue engineering has been evolved in the last decade and a myriad of scaffolding biomaterials and bioactive agents have been proposed. Controlled release of growth factors encapsulated in the polymeric nanomaterials has been of interest notably for the repair of damaged articular cartilage. Here, we proposed an on-chip hydrodynamic flow focusing microfluidic approach for synthesis of alginate nanogels loaded with the transforming growth factor beta 3 (TGF-β3) through an ionic gelation method in order to achieve precise release profile of these bioactive agents during chondrogenic differentiation of mesenchymal stem cells (MSCs). Alginate nanogels with adjustable sizes were synthesized by fine-tuning the flow rate ratio (FRR) in the microfluidic device consisting of cross-junction microchannels. The result of present study showed that the proposed approach can be a promising tool to synthesize bioactive -loaded polymeric nanogels for applications in drug delivery and tissue engineering.

1. Introduction

Cartilage regeneration continues to be largely intractable due to its poor regenerative properties and absence of vascularization (Grässel & Lorenz, 2014). Today and despite extensive preclinical data, no approved therapy capable of restoring the healthy structure of damaged cartilage is clinically available. Over the past decades, a large body of strategies involving a combination of stem cells, new biomaterials, and bioactive agents have been proposed for this matter (Huey, Hu, & Athanasiou, 2012). Cellular therapy using chondrocytes, fibroblasts, and stem cells (i.e., mainly mesenchymal stem cells (MSCs)) has been widely studied in various investigations (Ankrum & Karp, 2010; Zhang et al., 2015). The most-studied source of MSCs is the bone marrow, though MSCs have also been isolated from fat tissue, periosteum, and perichondrium (Mackay et al., 1998; Pittenger et al., 1999). In addition to cells, several growth factors (i.e., transforming growth factor β (TGF-β) superfamily members TGF-β1 and -β3), involved in the development of cartilage, have been identified as factors significantly affecting the chondrogenic differentiation of MSCs (Indrawattana et al., 2004). This growth factor can stimulate MSCs differentiation into the chondrogenic cell line and produce functionalized proteins such as aggrecan or type II of collagen (Fortier, Barker, Strauss, McCarrel, & Cole, 2011; Park, Temenoff, Holland, Tabata, & Mikos, 2005). Nonetheless, the therapeutic potential is hampered due to the short half-lives or prompt diffusion of these factors (Putney, 1998). To meet these demands, a controlled release of growth factors is a decisive factor for the efficient differentiation of tissues. Encapsulation of growth factors into polymer-based materials can improve their efficiency and controlled release (Edelman, Mathiowitz, Langer, & Klagsbrun, 1991; Wang et al., 2009).

Three-dimensionally cross-linked polymeric networks with submicron size, known as nanogels, have been broadly used as carriers for delivery of growth factors and proteins (Jiang, Chen, Deng, Suuronen, & Zhong, 2014). Possessing the desirable characteristics of both nanoparticles and hydrogels, these nanogels can be used individually as a growth factor delivery system, or combined with a polymeric matrix or scaffolds for further development of tissue engineering goals (Fujioka-Kobayashi et al., 2012; Kim et al., 2018; Yang et al., 2014). To date, various kinds of polymeric nanogels have been proposed, among which

* Corresponding authors.
E-mail addresses: Mohamadnejad@ut.ac.ir (J. Mohammadnejad), soleim_m@modares.ac.ir (M. Soleimani).

https://doi.org/10.1016/j.carbpol.2019.115551
Received 2 May 2019; Received in revised form 26 October 2019; Accepted 28 October 2019
Available online 07 November 2019
0144-8617/

alginate has gained far more attention given its unique features such as ease of gelation and biocompatibility (Edelman et al., 1991).

Conventional fabrication of nanogels using bulk mixing results in extensive polydispersity in their size, affecting their functional applications. Further, their uncontrollable release limits their suitability for *in-situ* cellular/tissue delivery (Bazban-Shotorbani, Dashtimoghadam, Karkhaneh, Hasani-Sadrabadi, & Jacob, 2016; Majedi et al., 2014). In recent years, there have been surges of interest in microfluidics which have provided investigators with careful handling of liquids on a micro scale (Lashkaripour, Rodriguez, Ortiz, & Densmore, 2019). Using the microfluidic approach, nanogels with a narrow size distribution can be generated through ionic gelation, which occurs via hydrodynamic flow-focusing of two miscible fluids in a continuous manner (Rhee et al., 2011). Ionic gelation is a simple yet viable method for crosslinking alginate under ambient conditions without applying any chemical additives or harsh conditions, which is important for the growth factor delivery. These benefits aid microfluidics to become a robust approach for the synthesis of size-control nanogels as well as for encapsulation of certain materials such as antibodies, cells, or proteins (Mahmoodi et al., 2019; Oh, Drumright, Siegwart, & Matyjaszewski, 2008). For the first time, Karnik et al. reported producing the controlled synthesis of monodispersed polymeric nanoparticles through microfluidic flow-focusing by convective-diffusive mixing (Karnik et al., 2008). Since then, several microfluidic flow-focusing devices have been developed for production of polymeric nanoparticles and nanogels. Overall, of the studies in the literature suggested that the device geometry, volumetric flow rate, and initial polymer concentration are of great importance regarding the size distribution of nanoparticles/nanogels (Chen, Zhang, Shi, Wu, & Hanagata, 2014; Feng et al., 2015; Rhee et al., 2011). Since the flow behavior is the most influential parameter in monodispersity of nanogels, one can make a library of various size nanogels by adjusting the key factors such as flow rate ratio (FRR) and initial polymer concentration (Amrani & Tabrizian, 2018). In this regard, recently, many studies have focused on encapsulation of TGF-β3 in hydrogels and nanogels (Bian et al., 2011; Erndt-Marino et al., 2018); however, control of burst release has still remained a challenge. Thus, more comprehensive investigations are required to fine-tune the parameters involved in the fabrication, storage, and *in-vivo* delivery. In this work, we studied the key parameters affecting the loading of TGF-β3 in alginate nanogels using a co-flow microfluidic system. Initially, we needed to investigate the effect of FRRs on the physiochemical characteristics of produced nanoparticles such as monodispersity and loading capacity. To do this more systematically, we employed CFD to model the flow behavior inside microchannels and obtain the best operating parameters for the production of polymeric nanogels. The sizes of the alginate nanoparticles were characterized by dynamic light scattering (DLS) method. Further, the encapsulation efficiency, release behavior, and cytotoxicity tests were performed for all synthesized nanogels to find the best performing nanoparticles. Eventually, our best performing nanoparticles were used to treat MSCs *ex-vivo* and assess the chondrogenic differentiation using a panel of genes via real-time PCR analysis method.

2. Materials and methods

2.1. Microchip design and fabrication

To fabricate the microfluidic chip, its pattern was drawn in SolidWorks 2016 (SolidWorks Corp), a powerful CAD and CAE program. The T-junction microfluidic device consisting of three inlets and one outlet was designed. The dimensions of the microchannels were 60 μm 120 μm and 1 cm in height, width, and length, respectively. This design was printed by a high-resolution printer, and a chrome mask was created. Then, SU-8 100 photoresist (Sigma-Aldrich) with a height of 3 mm was centrifuged on a silicon wafer. This SU-8 was baked 2 min to attach to the silicon wafer. Thereafter, the chrome mask was transferred on the SU-8 and exposed to UV lights. Ethyl oxalate was applied to clean the regions affected by UV lights. The mixture of PDMS with its curing agent (SILGARD 184, Dow Corning) at a ratio of 9:1 was poured on the created mask, degassed by a vacuum machine, and cured at the temperature of 60–65 °C for 2 h. The designed microchip was readily detached from the SU-8 and bounded by oxygen plasma (Plasma Etch) on a glass.

2.2. Synthesis of nanogels and encapsulation of TGF-β3

Synthesis of alginate nanogels was performed both by bulk and microfluidic methods. In the bulk approach, an alginate solution (Mn = 208,000 g.mol^{-1}, M/G = 1.2, Sigma-Aldrich) in water (1 mg.ml^{-1}) was added dropwise to $CaCl_2$ solution (Sigma-Aldrich, 10 mM) under constant stirring. In order to synthesize the growth factor-loaded nanogels, TGF-β3 (1 μg/ml, Sigma-Aldrich) was mixed with the alginate aqueous solution. For synthesis via the microfluidic approach, an alginate aqueous solution as core flow (1 mg.ml^{-1}) was injected into the microchip. At the same time, $CaCl_2$ as the sheath flow, was injected into the side channels' inlets of microchip. FRR described as the core flow to the sheath flow ratio was adjusted by a syringe pump. The sheath flows rate was kept constant in 3 ml/h (this number divided by tow for each side flow) and the core flow rate changed from 0.03 ml/h to 0.6 ml/h to obtain 0.01 to 0.2 FRRs. During this process, the core flow was squeezed by the sheath flows possessing a higher velocity. This led to rapid diffusion mixing of precursors followed by alginate ionic gelation. Nanogels were formed through the interaction of Ca^{2+} ions with alginate polymer chains functioning as a negative polyelectrolyte. Once the first nanogel nucleus was formed, it started to grow through adding more Ca^{2+} and polymer chain. In order to obtain synthesized TGF-β3 loaded within nanogels, it was first dissolved with water and then mixed with the alginate solution. This solution was then introduced into the microchip as the core flow. The suspension of alginate nanogels was collected followed by washing and redispersion in deionized water.

2.3. Dynamic light scattering (DLS) analysis

The size distribution and the corresponding zeta potential of alginate nanogels in the solution were identified via DLS method. The solution which was diluted in water was analyzed by Zetasizer (3000HS, Malvern Instrument Ltd, Worcestershire, UK).

2.4. Numerical simulation setting

In order to better understand the 3D behavior of the flow inside the microchip with different FRRs, the fluid flow was simulated by COMSOL Multiphysics 5.3a (COMSOL, Inc), commercially available software based on finite element method (FEM). Eqs. (1) to (3), being the continuity, Navier-Stokes, and convection-diffusion equations, have been coupled to simulate the fluid behavior (Bazaz et al., 2018).

$$\nabla . \boldsymbol{V} = 0 \tag{1}$$

$$\frac{\partial \boldsymbol{V}}{\partial t} + \rho(\boldsymbol{V}. \nabla)\boldsymbol{V} = -\nabla P + \mu\nabla^2\boldsymbol{V} \tag{2}$$

$$\frac{\partial c}{\partial t} + (\boldsymbol{V}. \nabla)c = \frac{1}{Re.\ Sc}\nabla^2 c \tag{3}$$

Where, $\boldsymbol{V}$ is considered as the velocity vector, P is assumed to be the fluid pressure, and c represents the concentration of two fluids. Also, Sc indicating the momentum diffusivity to mass diffusivity is the Schmidt number can be expressed by Eq. (4).

$$\mathrm{Sc} = \frac{\nu}{D} \tag{4}$$

Here, ν is the kinematic viscosity and D is diffusion coefficient rate. All velocities have been adjusted by Re number as proposed by Eq. (5) (Mollajan, Bazaz, & Mehrizi, 2018).

$$\mathrm{Re}=\frac{\rho V D_h}{\mu} \quad (5)$$

Where, μ is the dynamic viscosity, ρ denotes the density, and D_h shows the hydraulic diameter which can be calculated by 4A/ P, where A is the area cross section and P is the wetted perimeter. As the carrier flow mostly contained water, we chose its properties at room temperature for our numerical simulations.

The fluid was considered to be Newtonian, steady-state, and incompressible. The velocity and pressure boundary conditions were applied as the inlets and outlet, respectively (Rasouli, Mehrizi, Goharimanesh, Lashkaripour, & Bazaz, 2018).

2.5. Encapsulation efficiency and in vitro release

For calculating the value of TGF-β3 which was released from alginate nanogels in two weeks, a standard weight of the nanogels (10 mg) was picked and placed into micro tubes, after which 1.5 ml of phosphate buffer solution was added (PBS, Sigma-Aldrich). The micro tubes were then agitated at 37 °C and 8 rpm. At certain time points, the micro tubes were collected from the incubator, and enough time was given to natural nanoparticles to settle at the bottom of the tube. Thereafter, supernatants were collected and stored at -20 °C. ELISA assays kit (R&D systems) was employed for further investigation on the supernatant. For calculating the encapsulation efficiency, fresh alginate nanogels were dissolved in the sodium citrate solution (Sigma-Aldrich, 55 mM). Also, the encapsulation efficiency was calculated by normalizing the detected amount of TGF-β3 to the total amount of TGF-β3, which was used for the fabrication process of the nanogels which was 1 μg.

2.6. Isolation of human mesenchymal stem cells and characterization

Human mesenchymal stem cells (hMSCs) were extracted from the bone marrow aspirate of one healthy 40-year-old male donor according to the method previously described (Oraee-Yazdani et al., 2016; Yazdani et al., 2013). The bone marrow was obtained from the iliac crest after receiving written consent from the donor. Primary hMSCs were then expanded in cell culture media containing low-glucose Dulbecco's modified Eagle's medium (DMEM-LG; Sigma-Aldrich), 10 % fetal bovine serum (FBS; Fisher Scientific, Waltham, MA), and 1 % penicillin/streptomycin (P/S; Fisher Scientific) in a humidified atmosphere with 5 % CO_2 at 37 °C. For cell characterization of hMSCs, the cells were detached after three passages, and the expression of specific cell surface markers such as CD46, CD73, CD 90, and CD105 was verified by a flow cytometer (Partec, Switzerland) using the Flomax software. The flow cytometry analysis results have been presented in Fig. S1 (Please refer to electronic supporting information (ESI)).

2.7. Cytotoxicity analysis

An MTT assay was used to determine the cytotoxicity of the unloaded alginate nanogels. hMSCs were seeded in a 96-well plate with a density of 10,000 cells per well in triplicate. hMSCs were cultured in cell culture media and placed into an incubator at 37 °C with 5 % CO_2 supplied. After the cells were adhered to the plate, the synthesized alginate nanogels were mixed with cells across a variety of concentrations (50–800 μg/ml). The cell viability was measured using the MTT kit after 24 h. Different concentrations of nanogels were tested to assess the toxicity through multiple experiments. The untreated MSCs were considered as a control group.

2.8. Chondrogenic differentiation of hMSCs

The isolated hMSCs were expanded up to three passages in the cell culture media. Afterwards, hMSCs were cultured in a plate and the synthesized nanogels (i.e., manufactured either by microfluidic or bulk approach) were added to the standard chondrogenic differentiation media which comprised of cell culture medium, plus 10^{-7}M dexamethasone, Sigma-Aldrich, (causing enhanced gene expression of cartilage matrix component such as aggrecan) (Derfoul, Perkins, Hall, & Tuan, 2006), and 50 mg/ml ascorbate, Sigma-Aldrich, (which can lead to chondrocyte matrix production) (Farquharson, Berry, Mawer, Seawright, & Whitehead, 1998), without TGF-β3 (mediated upregulation of collagen type II and cartilage oligomeric matrix protein) and replaced three times a week.

2.9. Real-time PCR analysis

Chondrogenesis was further analyzed after two weeks of culturing through extraction of RNA by the manufacturer's protocol using Trizol reagent (Invitrogen, USA). This was followed by converting RNA to cDNA via Maxima H minus Firs Strand cDNA Synthesis kit (Thermo Scientific). Real-time quantitative polymerase chain reaction (qPCR) was carried out on a Piko real-time PCR (Thermo Scientific) system using Power up SYBER green Master Mix (Thermo Scientific), whereby the expressions of Sox9, Collagen type Π (COL2), and Aggrecan were evaluated. For the housekeeping gene, Beta-actin was utilized (For primer sequences, please refer to electronic supplementary information, (ESI)). The PCR process was undertaken with its specific protocol which was 1 min at 95 °C, followed by 40 amplification cycles for 15 s at 95 °C, 15 s at 60 °C, and 45 s at 72 °C. The transcript was normalized to the mean value of Beta-actin, and afterwards, ΔΔCt method was used for qualifying the relative expression.

2.10. Statistical analysis

All experiments were repeated at least three times. All data were represented with the standard format of mean ± standard deviation. To determine the statistical significance, a *t*-test was used and the differences were assumed to be significant if $^*p < 0.05$.

3. Results and discussions

3.1. Hydrodynamic diameter results and mixing time calculation

As displayed in Fig. 1A, the microfluidic flow focusing chip employed in this study for the size-controlled production of nanogels consisted of three inlets. Two horizontal side channels were used as inlets for the $CaCl_2$ delivery as the sheath flow, while the central channel was utilized as a core flow for alginate and TGF-β3 solution. The outlet channel was also prepared to extract the products. Precise control of the size and monodispersity of the nanogels is a key parameter for biomedical applications (Karnik et al., 2008). Microfluidic platform allows this control over a wide range of sizes. FRR gives researchers the opportunity of controlling the desired size of the nanogels; thus, in the present study, we investigated the effect of FRRs on the nanogel sizes. Based on our previous study (Mahmoodi et al., 2019), and the simulation results of the fluid behavior inside the microfluidic device, FRRs were set as 0.01, 0.05, 0.1, 0.15, and 0.2. The mean hydrodynamic diameter for the synthesized nanogels for FRRs was measured by DLS as presented in Fig. 1B. The results indicated that the nanogels synthesized by the microfluidic method were monodispersed with the average diameters of 43 ± 4, 58 ± 5, 76 ± 5, 94 ± 7, and 125 ± 7 nm, respectively for the above-mentioned FRRs. Further, bulk synthesized nanogels had a larger polydispersity index (PDI ≥ 0.5) compared to their microfluidic aided counterparts (PDI ≤ 0.2). In addition, the average diameter of nanogels for the bulk approach was 137 ± 22 nm, indicating that the nanogels were larger than the microfluidics synthesized ones even at the highest FRR. Also, the zeta potential for microfluidic synthesized nanogels was −43, −38, and −22 mV for FRRs 0.01, 0.05, and 0.2, while for the bulk synthesized case, it was −16 mV. Therefore, the microfluidic-based method was

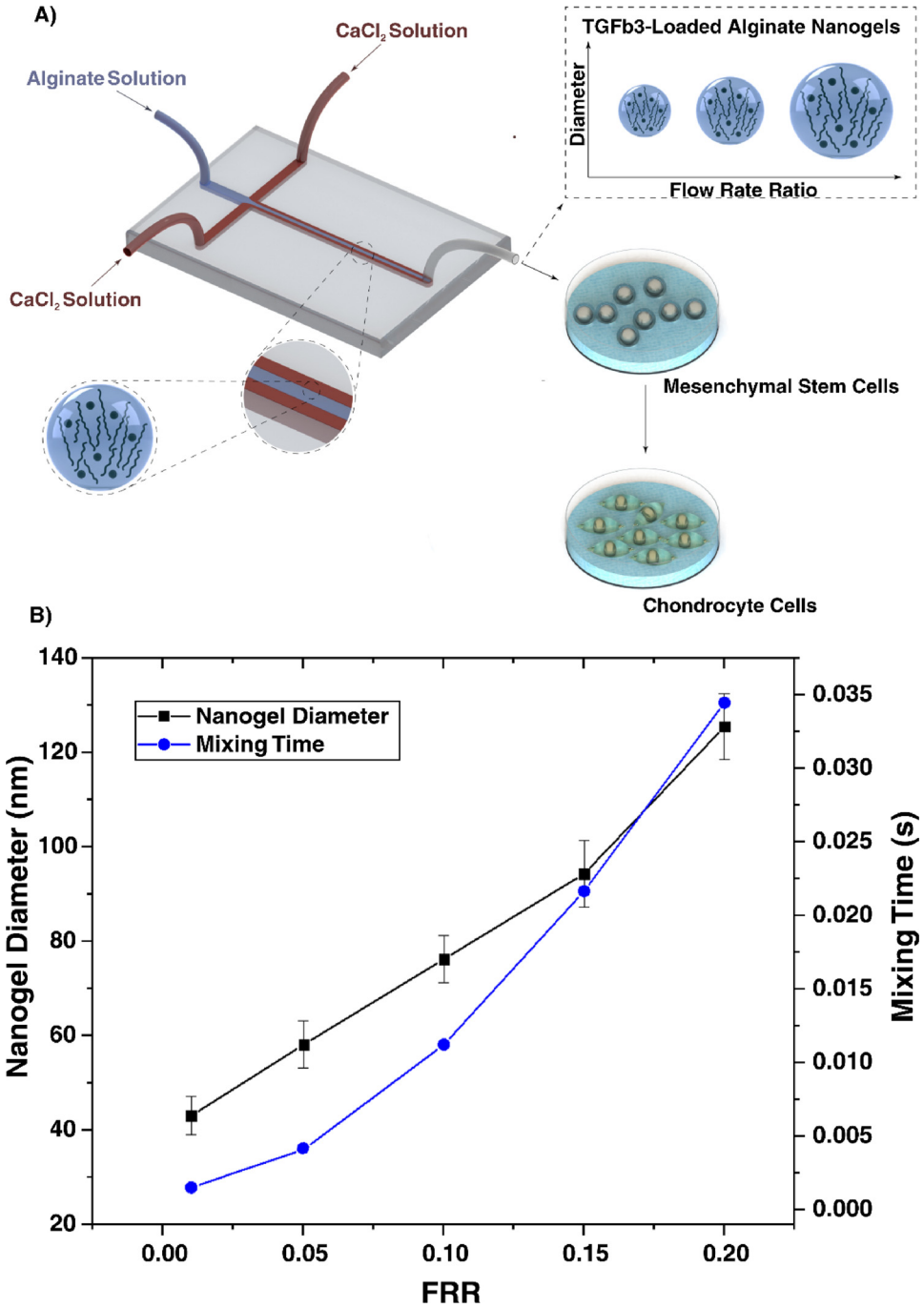

Fig. 1. a) Schematic illustration of microfluidic device for hydrodynamic flow-focusing consisting of one inlet for focusing (core) flow and two separate inlets for the sheath (side) flows; The chondrogenic differentiation potential of the synthesized nanogels loaded with TGF-β3 was then compared against an in vitro human mesenchymal stem cells model. b) The nanogels' diameter and mixing time against different FRRs; The diameter of the nanogels and the mixing time increased with the rise in the FRR. (The error bars indicate mean size ± stdev).

proven to generate size-tunable monodispersed nanogels with smaller diameters and a greater surface charge than the bulk ones did. Based on Eq. (6), the mixing time for different FRRs was calculated. (Where w represents the width of the channel (60 μm), and D is diffusivity of the calcium ions).

$$t_{mixing} \approx \frac{w^2}{9D} \times \frac{1}{\left(1 + \frac{1}{FRR}\right)^2} \quad (6)$$

The results presented in Fig. 1B indicated that alteration of FRR to 0.01, 0.05, 0.1, 0.15 and 0.2 resulted in mixing time variations from 0.121 ms to 0.0342 s (the diffusion coefficient was considered as $1.3 \times 10^{-9}\ m^2 s^{-1}$) (Bazban-Shotorbani et al., 2016). Also, based on the presented results, the longer the mixing time, the larger the nanogels, as confirmed by nanogels' DLS output (presented in Section 3.2).

Note that synthesis and characterization of nanoparticles and nanogels have been performed and evaluated in drug delivery systems and tissue engineering by the microfluidic method, with the outcomes of this study being consistent with those results (Karnik et al., 2008; Kim et al., 2012; Liu et al., 2015). The size distribution of the microfluidic-assisted fabricated nanogels in this study was among the lowest reported values for alginate nanogels produced in this molecular weight.

Generally, the bulk method generates nanogels under the condition

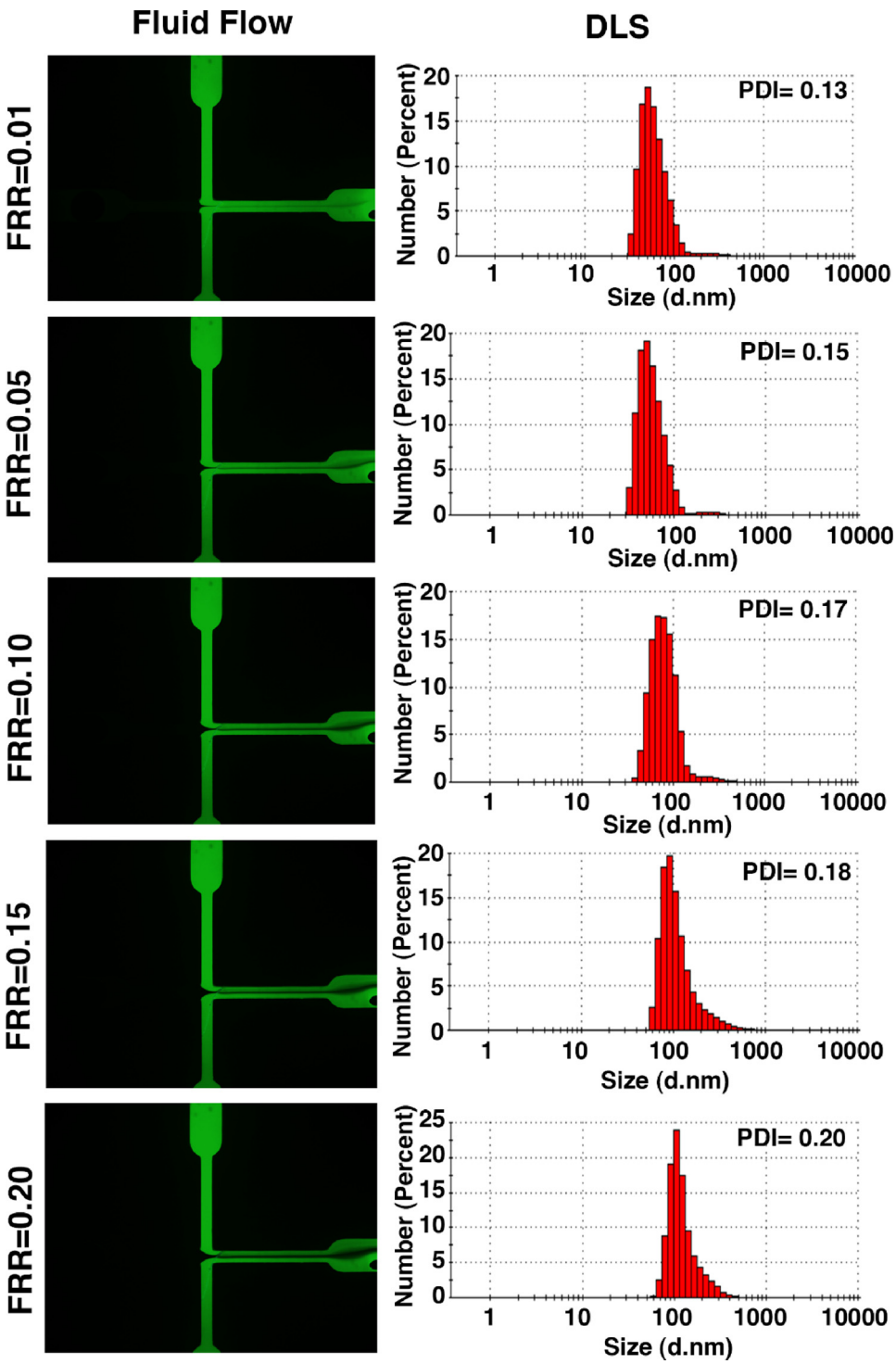

Fig. 2. Accordance of DLS result with hydrodynamic laminar flow in different FRRs using the developed microfluidic device. FRR = 0.01 (nanogels size = 43 ± 4 nm), FRR = 0.05 (nanogels size = 58 ± 5 nm), FRR = 0.1 (nanogels size = 76 ± 5 nm), FRR = 0.15 (nanogels size = 94 ± 7 nm) and FRR = 0.2 (nanogels size = 125 ± 7 nm).

of heterogenic reaction, and as a result, monodispersity is not feasible. On the other hand, FRR in a microfluidic approach is a dexterous toolbox enabling investigators to adjust the nanogel sizes by altering the FRR (Hasani-Sadrabadi et al., 2012; Mahmoodi, Bazaz, Mohammadnejad, Mehrizi, & Soleimani, 2016). The reason behind this fact is that the sheath flows can reduce the interfacial area of the core flow. Since the FRR and the inlet velocity of two side channels are stable during the experiment, monodispersed nanogels can be generated (Chen et al., 2014; Demello, 2006; Lim et al., 2014).

3.2. Consistency between FRRs and DLS results

Using fluorescein sodium salt (Sigma-Aldrich), which added to sheath flows, the images of hydrodynamic focused laminar flows were produced in every individual FRR and captured by fluorescence microscope (Nikon- eclipse 80i) as displayed in Fig. 2. Also, the results of DLS analysis have been indicated through the diagram of mean size percentage of the nanogels. These results broadly support each other and the expectation of different FRRs made by florescent dyes; it was

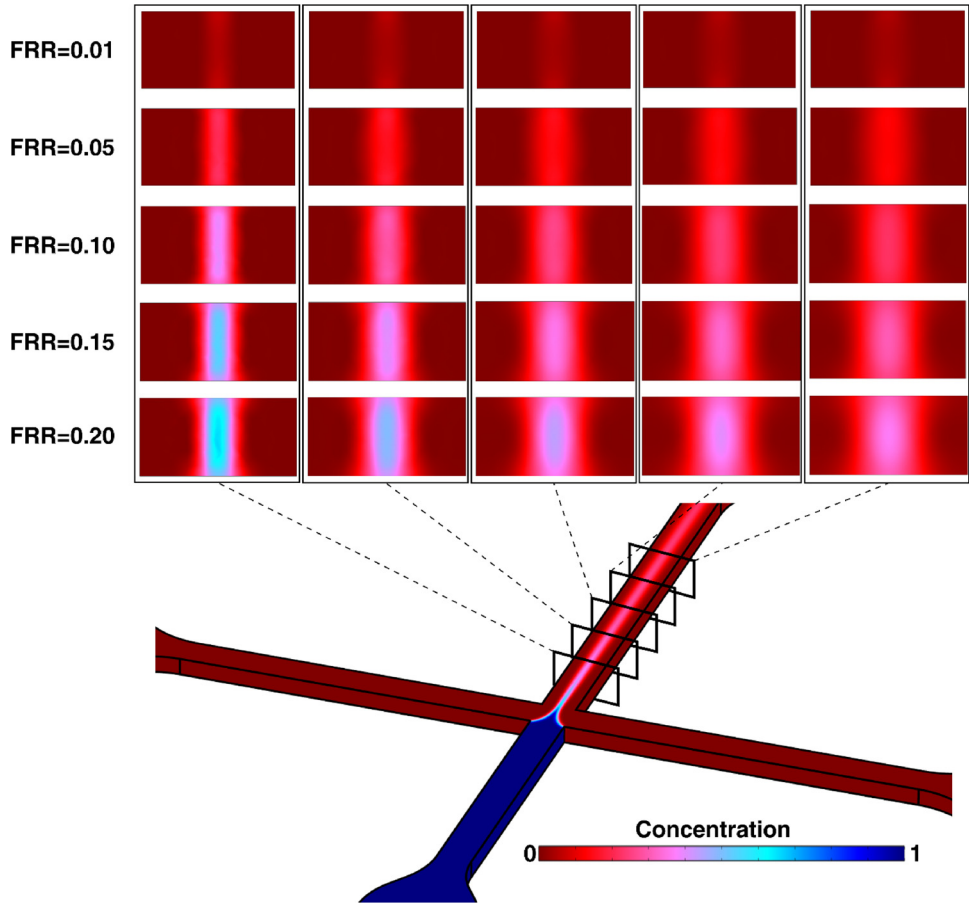

Fig. 3. Simulation results for various FRRs of 0.01, 0.05, 0.1, 0.15, and 0.20. In the legend bar, 0 and 1 mean no mixing while 0.5 refers to complete mixing.

mentioned that an increase in the FRR augments the nanogels' diameter.

3.3. Fluid behavior inside the microchannel

In order to gain a new insight into the flow behavior within the microchannel, the fluid flow inside the microchannel was simulated by finite element method, whose results are illustrated in Fig. 3. Various FRRs utilized in this study were evaluated. The beauty of simulation is that variations of concentration and velocity can easily be monitored without any advanced facilities or adroit users (Lashkaripour, Mehrizi, Goharimanesh, Rasouli, & Bazaz, 2018). In this simulation, the concentration of the core flow was considered to be 1, while the concentration of the sheath flow was assumed to be 0. As revealed in Fig. 3, for FRR of 0.01, the sheath flows thoroughly squeezed the core flow and shorter time was given to the core flow to be dispersed. Accordingly, the reason why the nanogels synthesized in this FRR had the minimum diameter is that the narrow width of the focused stream enabled two fluids to mix only in a limited width. As a result, once the mixing time was shortened, nanogels did not have enough time for aggregation formation ($\tau_{mix} < \tau_{agg}$), leading to synthesis of smaller nanogels which are expectedly more homogenous (Karnik et al., 2008). Compared to other FRRs, FRR of 0.2 had the maximum core flow velocity. Hence, the mixing occurred slower in comparison to the lower FRRs. As such, the gelation of particles occurred slower, leading to the formation of larger nanoparticles. As shown by the interfacial area of FRR of 0.2, nanogels with a larger diameter were generated. So, the higher the FRR, the lower the sheath flow velocity and thus the greater the nanoparticle diameter would be. In previous studies, the same pattern was observed for flow-focusing devices (Amrani & Tabrizian, 2018; Min, Im, Lee, & Kim, 2014; Rhee et al., 2011).

3.4. Encapsulation efficiency and cumulative release

Encapsulation efficiency can be represented by the fraction of entrapped TGF-β3 in synthesized nanogels to the initial amount of TGF-β3. The nanogels synthesized by the conventional bulk method which usually have a large pore size led to leaching of the cargo during preparation, thereby leading to burst release and low encapsulation efficiency (Bazban-Shotorbani et al., 2016; Soleimani et al., 2016). The encapsulation efficiency calculated in the present study was greater than 73 % for the nanogels synthesized at FRR of 0.01 which can be regarded as a high encapsulation efficiency. The encapsulation efficiency for the nanogels synthesized at FRRs of 0.05, 0.1, 0.15, and 0.2 was 68 %, 62 %, 55 %, and 50 %, respectively, while it was 45 % for the bulk synthesized cases. The higher encapsulation efficiency of microfluidics-synthesized nanogels can be attributed to the smaller pore size for on chip synthesized nanogels compared to the bulk ones. Previous works on microfluidics nanogels have indicated that these nanogels have a smaller pore size compared to their bulk synthesis counterparts (Bazban-Shotorbani et al., 2016; Bazban-Shotorbani et al., 2017).

The cumulative release of TGF-β3 at any time interval was normalized to the initial loaded drug in nanogels. Based on Fig. 4A, it is obvious that the release speed in the bulk approach nanogels was faster than in microfluidic nanogels. According to Fig. 4A, it can be seen that after two weeks, approximately 68 %, 73 %, 75 %, and 83 % of TGF-β3 were released from the microfluidics-based nanogels synthesized at FRRs 0.01, 0.05, 0.1, and 0.2, respectively, while for the bulk mixing nanogels, it was about 99 %. Thus, we can say that sustained release is more achievable via microfluidic synthesis approach. We also

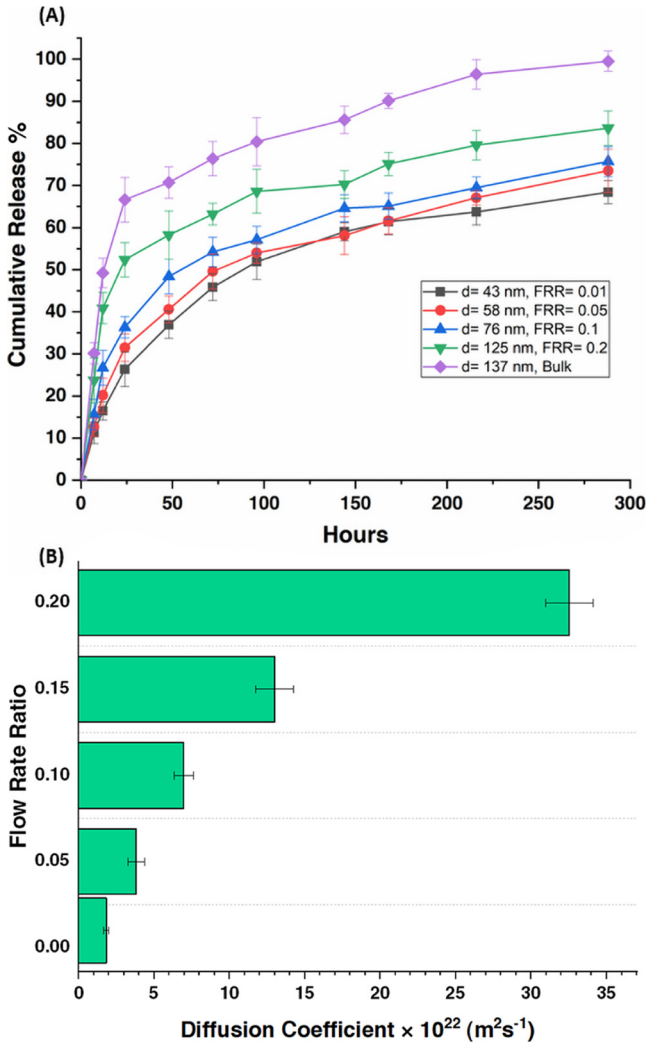

Fig. 4. a) Cumulative release of TGF-β3 encapsulated in alginate nanogels for two weeks; the release behavior was studied by different nanogel sizes across different FRRs. The cumulative release is based on the percentage of the TGF-β3 which has been released. Data are expressed as mean ± SD (n = 3); **b)** The number for the diffusion coefficients calculated based on fraction of TGF-β3 released from different series of the nanogels.

calculated the diffusion coefficient (Fig. 4B) for TGF-β3 for the nanogels according to Eq. 7, using the TGF-β3 release experimental data (Fig. 4a), and by fitting Eq.7 to those data, we succeeded to estimate the diffusion coefficient of TGF-β3, where Mt/MN represents the fraction of the released protein at time *t*, *D* denotes the diffusion coefficient of the TGF-β3 molecules, and R_h is the hydrodynamic radius of the particles. It is evident that the microfluidic nanoparticles presented considerably lower values of the diffusion coefficient.

$$\frac{M_t}{M_\infty} = 6\left(\frac{Dt}{\pi R_h^2}\right)^{1/2} \tag{7}$$

It is well-known that the drug release rate from nanoparticle matrices is mainly controlled by the diffusion rate of the drug out of nanogels' matrix (Romero-Cano & Vincent, 2002). Also, we know from previous works that rapid mixing in microfluidic approach results in more compact nanoparticles, and eventually in slower diffusion of the cargo out of nanoparticles' matrix (Hasani-Sadrabadi et al., 2015; Hasani-Sadrabadi et al., 2014; Vardar et al., 2018).

It is known that differentiation is a long and continuous process; the main aim of this study has been the differentiation of hMSCs into the chondrogenic phenotype. Indeed, this elongated release supports better differentiation (Bouffi et al., 2010; Re'em, Kaminer-Israeli, Ruvinov, & Cohen, 2012). Although we expect that nanoparticles with a larger diameter have a slower release due to their larger surface to volume ratio, Fig. 4 suggests that the release profile of TGF-β3 from nanogels has a direct relationship with the hydrodynamic diameter of nanogels, where the smaller the size of nanogels, the slower the TGF-β3 release would be. The reason behind this fact in that microfluidics synthesis method leads to more compact nanogels; so more compactness of smaller nanogels leads to a slower release profile. Overall, the amount and rate of TGF-β3 release have a direct relationship to the nanogels' diameter (Dashtimoghadam, Mirzadeh, Taromi, & Nyström, 2013), where this postulated scenario is completely appropriate for hMSCs differentiation.

3.5. MTT tests for cytotoxicity assay of Nanogels

In general, cell toxicity of a drug barrier hinders the progress of efficient drug delivery. Thus, it is of great importance to evaluate the cell viability of alginate nanogels via MTT test. Fig. 5 illustrates that at 37 °C and after 24 h, the nanogels synthesized either by microfluidic or conventional approach have been non-toxic. Based on Fig. 5, the low concentration of nanogels led to higher percentage of cell viability; also, by reducing the nanogels' diameters and increasing of surface charge, cell viability increased.

3.6. Chondrogenic marker gene expression

The potential of the released TGF-β3 in promoting chondrogenesis in hMSCs synthesized via microfluidic and bulk approach was evaluated within 14 days. Collagen type II, Sox9, and Aggrecan as three chondrogenesis gene markers were selected and evaluated by real-time PCR technique, with the results being presented in Fig. 6. Based on Fig. 6, through 14 days, the contents of gene expressions, normalized by Beta-actin RNA content, were compared across the groups of cells which had been treated with encapsulated TGF-β3 and control group which was free TGF-β3. The real-time PCR results revealed that chondrogenic marker genes expressions for encapsulated TGF-β3 were significantly higher than in the control group. Also, the microfluidic-synthesized nanogels loaded with TGF-β3 were more extensive than the bulk mode loaded nanogels.

As shown in Fig. 6A, upregulation of Sox9, which is a dominant regulator of chondrogenic differentiation, was discernible, and the nanogels synthesized via the microfluidic approach had a higher chondrogenic differentiation potential compared to the nanogels synthesized via bulk method. Further, Collagen type II and Aggrecan are the main collagen fibers of cartilage tissue and the major cartilage comprising proteoglycan respectively. Therefore, mRNA expression of these genes was assumed to be the primary marker for chondrogenic differentiation. Based on Fig. 6, the expression of Collagen type II and Aggrecan significantly increased compared to the control group with the augmentation value being greater in microfluidic-based nanogels compared to their bulk-based counterparts.

One possible explanation for higher chondrogenic gene expression in microfluidics-based nanogels in comparison to nanogels synthesized in the bulk approach can be associated with the smaller pore size of the microfluidic synthesized nanogels. As illustrated by previous studies which have focused on microfluidics synthesis of nanogels, the release rate is directly related to the pore size of nanogels (Bazban-Shotorbani et al., 2017; Soleimani et al., 2016). According to the study conducted by Bazban-Shotorban et al., the smaller the pore of the synthesized nanogels, the slower the release of the protein will be (Bazban-Shotorbani et al., 2016). Furthermore, Hasani-Sadrabadi et al. demonstrated that microfluidics synthesized nanoparticles are more compact compared to bulk nanoparticles. This leads to minimum burst release and sustained release of growth factor into the culture medium causing

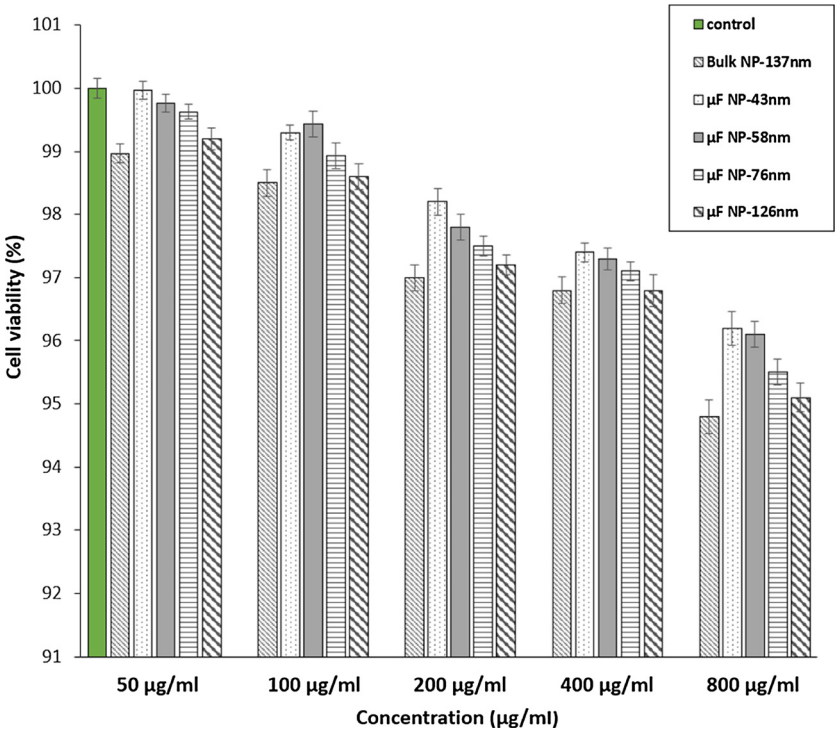

Fig. 5. The percentage of the cell viability of unloaded alginate-nanogels in different sizes and various concentrations after 24 h incubation. Data represent mean ± SD and expressed as cell viability percent (n = 3), we used untreated MSCs as control group.

a better differentiation as represented in the microfluidic-based nanogels (Hasani-Sadrabadi et al., 2015). Also, according to our results, microfluidics produced nanogels with a smaller size had more chondrogenic differentiation potentials. As previously illustrated in this study, nanogels with a smaller size had a lower diffusion coefficient which could lead to slowed release of TGF-β3 compared to nanogels with a larger size (Hasani-Sadrabadi et al., 2015).

Previously, many attempts were made for TGF-β3 spatiotemporal controlled release for chondrogenic tissue engineering both *in vitro* and *in vivo* (Böck et al., 2018; Chiang et al., 2018; Crecente-Campo, Borrajo, Vidal, & Garcia-Fuentes, 2017). Specifically, many studies have focused on encapsulation of growth factors in hydrogels for tissue engineering (Fujioka-Kobayashi et al., 2012). Recently, Hou and his colleagues were able to generate microgels from PVA polymer using the microfluidic approach. The controlled release of TGF-β3 of those microgels could efficiently enhance chondrogenic differentiation of hMSCs (Hou et al., 2018). It was also proposed that *in vitro* upregulation of chondrogenic gene expression via MCSs was substantial in the presence of TGF-β3 encapsulated by PLGA particles nanoparticles. In addition, it was reported that the regeneration of articular cartilage was improved in rabbit humeral joints by TGF-β3 transported in the collagen hydrogel. In this article, we observed that the controlled release of TGF-β3 from microfluidic-based nanogels led to enhanced chondrogenic gene expression compared to the bulk-based nanogels. The nanogels synthesized in this study had diameter less than 100 nm. This feature make them ideal candidates to be injected for cartilage tissue engineering (Ren et al., 2016).

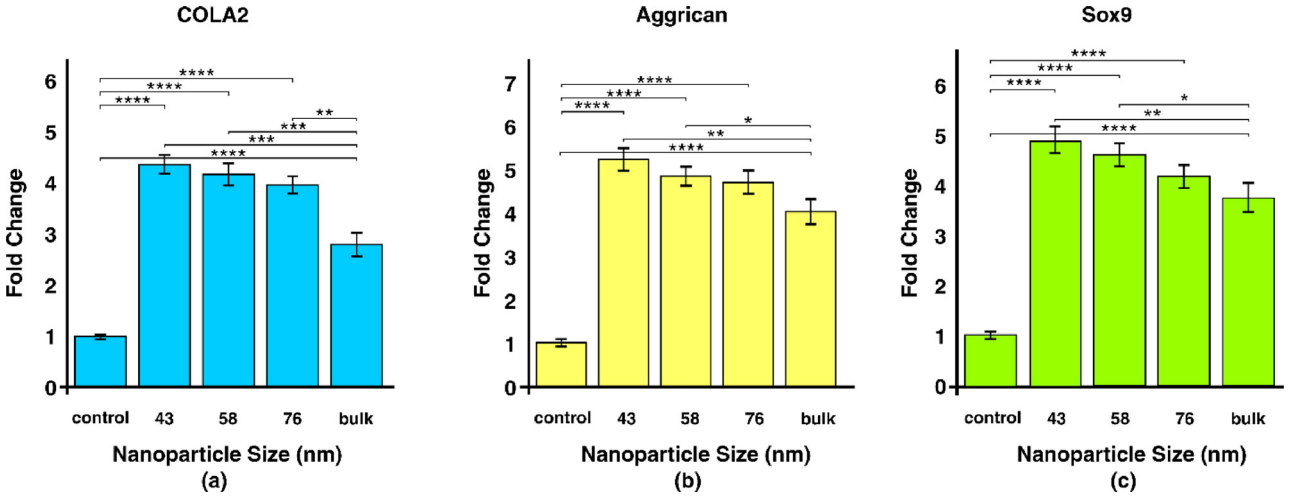

Fig. 6. Effect of the microfluidics and bulk synthesized TGF-β3 loaded alginate nanogels on chondrogenic marker genes expression using human mesenchymal stem cells (hMSCs), *in vitro* model; Representative charts (a–c) indicate relative mRNA levels of COLA2 (a), Aggrecan (b), and Sox9 (c) in cells normalized with mRNA of Beta-actin in the same sample using real-time PCR. hMSCs were used as the control sample. Values indicate mean ± SD. *P ≤ 0.05, **P ≤ 0.01, and ***P ≤ 0.001.

4. Conclusion

In the present study, we proposed a simple yet practical approach for manufacturing of alginate nanogels using a co-flow microfluidic chip. We utilized CFD simulation to study the flow behavior inside the microchannels and optimize the FRRs. By adjusting the FRR, we were able to control the main physical properties of the resulted nanogels, including the size and cargo release rate. DLS results revealed that average diameters of 43 ± 4–125 ± 7 nm were achieved in FRRs of 0.01 to 0.2. We observed that the microfluidic-synthesized nanogels have a smaller size and higher monodispersity compared to conventional bulk synthesized nanogels. Besides, a sustained release behavior for TGF-β3 was achieved by employing these uniform-size nanogels and, hence, the burst release was significantly reduced. To investigate the *in-vitro* behavior of the synthesized nanogels, the effect of TGF-β3-loaded alginate nanogels on the chondrogenic differentiation of MSCs was examined. Based on the obtained results, microfluidic synthesized nanogels showed superior performance in terms of uniform release of TGF-β3 molecules, resulting in better chondrogenic differentiation of MSCs which are confirmed with the PCR analysis. In summary, we have developed a system which can be a promising tool to synthesize growth factor-loaded polymeric nanogels for applications in diverse cell and tissue engineering.

Appendix A. Supplementary data

Supplementary material related to this article can be found, in the online version, at doi:https://doi.org/10.1016/j.carbpol.2019.115551.

References

Amrani, S., & Tabrizian, M. (2018). Characterization of nanoscale loaded liposomes produced by 2D hydrodynamic flow focusing. *ACS Biomaterials Science & Engineering, 4*(2), 502–513.

Ankrum, J., & Karp, J. M. (2010). Mesenchymal stem cell therapy: Two steps forward, one step back. *Trends in Molecular Medicine, 16*(5), 203–209.

Bazaz, S. R., Mehrizi, A. A., Ghorbani, S., Vasilescu, S., Asadnia, M., & Warkiani, M. E. (2018). A hybrid micromixer with planar mixing units. *RSC Advances, 8*(58), 33103–33120.

Bazban-Shotorbani, S., Dashtimoghadam, E., Karkhaneh, A., Hasani-Sadrabadi, M. M., & Jacob, K. I. (2016). Microfluidic directed synthesis of alginate nanogels with tunable pore size for efficient protein delivery. *Langmuir, 32*(19), 4996–5003.

Bazban-Shotorbani, S., Hasani-Sadrabadi, M. M., Karkhaneh, A., Serpooshan, V., Jacob, K. I., Moshaverinia, A., et al. (2017). Revisiting structure-property relationship of pH-responsive polymers for drug delivery applications. *Journal of Controlled Release, 253*, 46–63.

Bian, L., Zhai, D. Y., Tous, E., Rai, R., Mauck, R. L., & Burdick, J. A. (2011). Enhanced MSC chondrogenesis following delivery of TGF-β3 from alginate microspheres within hyaluronic acid hydrogels in vitro and in vivo. *Biomaterials, 32*(27), 6425–6434.

Böck, T., Schill, V., Krähnke, M., Steinert, A. F., Tessmar, J., Blunk, T., et al. (2018). TGF-β1-Modified hyaluronic Acid/Poly (glycidol) hydrogels for chondrogenic differentiation of human mesenchymal stromal cells. *Macromolecular Bioscience, 18*(7), 1700390.

Bouffi, C., Thomas, O., Bony, C., Giteau, A., Venier-Julienne, M. C., Jorgensen, C., Montero-Menei, C., & Noel, D. (2010). The role of pharmacologically active microcarriers releasing TGF-beta3 in cartilage formation in vivo by mesenchymal stem cells. *Biomaterials, 31*(25), 6485–6493.

Chen, S., Zhang, H., Shi, X., Wu, H., & Hanagata, N. (2014). Microfluidic generation of chitosan/CpG oligodeoxynucleotide nanoparticles with enhanced cellular uptake and immunostimulatory properties. *Lab on a Chip, 14*(11), 1842–1849.

Chiang, C.-S., Chen, J.-Y., Chiang, M.-Y., Hou, K.-T., Li, W.-M., Chang, S.-J., et al. (2018). Using the interplay of magnetic guidance and controlled TGF-β release from protein-based nanocapsules to stimulate chondrogenesis. *International Journal of Nanomedicine, 13*, 3177.

Crecente-Campo, J., Borrajo, E., Vidal, A., & Garcia-Fuentes, M. (2017). New scaffolds encapsulating TGF-β3/BMP-7 combinations driving strong chondrogenic differentiation. *European Journal of Pharmaceutics and Biopharmaceutics, 114*, 69–78.

Dashtimoghadam, E., Mirzadeh, H., Taromi, F. A., & Nyström, B. (2013). Microfluidic self-assembly of polymeric nanoparticles with tunable compactness for controlled drug delivery. *Polymer, 54*(18), 4972–4979.

Demello, A. J. (2006). Control and detection of chemical reactions in microfluidic systems. *Nature, 442*(7101), 394.

Derfoul, A., Perkins, G. L., Hall, D. J., & Tuan, R. S. (2006). Glucocorticoids promote chondrogenic differentiation of adult human mesenchymal stem cells by enhancing expression of cartilage extracellular matrix genes. *Stem Cells, 24*(6), 1487–1495.

Edelman, E. R., Mathiowitz, E., Langer, R., & Klagsbrun, M. (1991). Controlled and modulated release of basic fibroblast growth factor. *Biomaterials, 12*(7), 619–626.

Erndt-Marino, J. D., Jimenez-Vergara, A. C., Diaz-Rodriguez, P., Kulwatno, J., Diaz-Quiroz, J. F., Thibeault, S., et al. (2018). In vitro evaluation of a basic fibroblast growth factor-containing hydrogel toward vocal fold lamina propria scar treatment. *Journal of Biomedical Materials Research Part B, Applied Biomaterials, 106*(3), 1258–1267.

Farquharson, C., Berry, J. L., Mawer, E. B., Seawright, E., & Whitehead, C. C. (1998). Ascorbic acid-induced chondrocyte terminal differentiation: The role of the extracellular matrix and 1, 25-dihydroxyvitamin D. *European Journal of Cell Biology, 76*(2), 110–118.

Feng, Q., Zhang, L., Liu, C., Li, X., Hu, G., Sun, J., et al. (2015). Microfluidic based high throughput synthesis of lipid-polymer hybrid nanoparticles with tunable diameters. *Biomicrofluidics, 9*(5), 052604.

Fortier, L. A., Barker, J. U., Strauss, E. J., McCarrel, T. M., & Cole, B. J. (2011). The role of growth factors in cartilage repair. *Clinical Orthopaedics and Related Research, 469*(10), 2706–2715.

Fujioka-Kobayashi, M., Ota, M. S., Shimoda, A., Nakahama, K.-i., Akiyoshi, K., Miyamoto, Y., et al. (2012). Cholesteryl group-and acryloyl group-bearing pullulan nanogel to deliver BMP2 and FGF18 for bone tissue engineering. *Biomaterials, 33*(30), 7613–7620.

Grässel, S., & Lorenz, J. (2014). Tissue-engineering strategies to repair chondral and osteochondral tissue in osteoarthritis: use of mesenchymal stem cells. *Current Rheumatology Reports, 16*(10), 452.

Hasani-Sadrabadi, M. M., Hajrezaei, S. P., Emami, S. H., Bahlakeh, G., Daneshmandi, L., Dashtimoghadam, E., Seyedjafari, E., Jacob, K. I., & Tayebi, L. (2015). Enhanced osteogenic differentiation of stem cells via microfluidics synthesized nanoparticles. *Nanomedicine Nanotechnology Biology and Medicine, 11*(7), 1809–1819.

Hasani-Sadrabadi, M. M., Majedi, F. S., VanDersarl, J. J., Dashtimoghadam, E., Ghaffarian, S. R., Bertsch, A., Moaddel, H., & Renaud, P. (2012). Morphological tuning of polymeric nanoparticles via microfluidic platform for fuel cell applications. *Journal of the American Chemical Society, 134*(46), 18904–18907.

Hasani-Sadrabadi, M. M., Karimkhani, V., Majedi, F. S., Van Dersarl, J. J., Dashtimoghadam, E., Afshar-Taromi, F., Mirzadeh, H., Bertsch, A., Jacob, K. I., & Renaud, P. (2014). Microfluidic-assisted self-assembly of complex dendritic polyethylene drug delivery nanocapsules. *Advanced Materials, 26*(19), 3118–3123.

Hou, Y., Xie, W., Achazi, K., Cuellar-Camacho, J. L., Melzig, M. F., Chen, W., et al. (2018). Injectable degradable PVA microgels prepared by microfluidic technology for controlled osteogenic differentiation of mesenchymal stem cells. *Acta Biomaterialia, 77*, 28–37.

Huey, D. J., Hu, J. C., & Athanasiou, K. A. (2012). Unlike bone, cartilage regeneration remains elusive. *Science, 338*(6109), 917–921.

Indrawattana, N., Chen, G., Tadokoro, M., Shann, L. H., Ohgushi, H., Tateishi, T., Tanaka, J., & Bunyaratvej, A. (2004). Growth factor combination for chondrogenic induction from human mesenchymal stem cell. *Biochemical and Biophysical Research Communications, 320*(3), 914–919.

Jiang, Y., Chen, J., Deng, C., Suuronen, E. J., & Zhong, Z. (2014). Click hydrogels, microgels and nanogels: Emerging platforms for drug delivery and tissue engineering. *Biomaterials, 35*(18), 4969–4985.

Karnik, R., Gu, F., Basto, P., Cannizzaro, C., Dean, L., Kyei-Manu, W., Langer, R., & Farokhzad, O. C. (2008). Microfluidic platform for controlled synthesis of polymeric nanoparticles. *Nano Letters, 8*(9), 2906–2912.

Kim, T.-H., Yun, Y.-P., Shim, K.-S., Kim, H.-J., Kim, S. E., Park, K., et al. (2018). In vitro anti-inflammation and chondrogenic differentiation effects of inclusion nanocomplexes of hyaluronic acid-beta cyclodextrin and simvastatin. *Tissue Engineering and Regenerative Medicine, 15*(3), 263–274.

Kim, Y., Lee Chung, B., Ma, M., Mulder, W. J., Fayad, Z. A., Farokhzad, O. C., et al. (2012). Mass production and size control of lipid–polymer hybrid nanoparticles through controlled microvortices. *Nano Letters, 12*(7), 3587–3591.

Lashkaripour, A., Mehrizi, A. A., Goharimanesh, M., Rasouli, M., & Bazaz, S. R. (2018). Size-controlled droplet generation in a microfluidic device for rare dna amplification by optimizing its effective parameters. *Journal of Mechanics in Medicine and Biology, 18*(01), 1850002.

Lashkaripour, A., Rodriguez, C., Ortiz, L., & Densmore, D. (2019). Performance tuning of microfluidic flow-focusing droplet generators. *Lab on A Chip, 19*(6), 1041–1053.

Lim, J. M., Swami, A., Gilson, L. M., Chopra, S., Choi, S., Wu, J., Langer, R., Karnik, R., & Farokhzad, O. C. (2014). Ultra-high throughput synthesis of nanoparticles with homogeneous size distribution using a coaxial turbulent jet mixer. *ACS Nano, 8*(6), 6056–6065.

Liu, D., Cito, S., Zhang, Y., Wang, C. F., Sikanen, T. M., & Santos, H. A. (2015). A versatile and robust microfluidic platform toward high throughput synthesis of homogeneous nanoparticles with tunable properties. *Advanced Materials, 27*(14), 2298–2304.

Mackay, A. M., Beck, S. C., Murphy, J. M., Barry, F. P., Chichester, C. O., & Pittenger, M. F. (1998). Chondrogenic differentiation of cultured human mesenchymal stem cells from marrow. *Tissue Engineering, 4*(4), 415–428.

Mahmoodi, L., Bazaz, S. R., Mohammadnejad, J., Mehrizi, A. A., & Soleimani, M. (2016). Size-tunable alginate nanoparticles synthesis using T-junction microfluidic chip. *IEEE 2016 23rd Iranian Conference on Biomedical Engineering and 2016 1st International Iranian Conference on Biomedical Engineering (ICBME)*.

Mahmoodi, Z., Mohammadnejad, J., Bazaz, S. R., Mehrizi, A. A., Ghiass, M. A., Saidijam, M., Dinarvand, R., Warkiani, M. E., & Soleimani, M. (2019). A simple coating method of PDMS microchip with PTFE for synthesis of dexamethasone-encapsulated PLGA nanoparticles. *Drug Delivery and Translational Research, 9*(3), 707–720.

Majedi, F. S., Hasani-Sadrabadi, M. M., VanDersarl, J. J., Mokarram, N., Hojjati-Emami, S., Dashtimoghadam, E., Bonakdar, S., Shokrgozar, M. A., Bertsch, A., & Renaud, P. (2014). Drug delivery: On-chip fabrication of paclitaxel-loaded chitosan nanoparticles for Cancer therapeutics. *Advanced Functional Materials, 24*(4), 418 4/2014.

Min, K.-I., Im, D. J., Lee, H.-J., & Kim, D.-P. (2014). Three-dimensional flash flow microreactor for scale-up production of monodisperse PEG–PLGA nanoparticles. *Lab on a Chip, 14*(20), 3987–3992.

Mollajan, M., Bazaz, S. R., & Mehrizi, A. A. (2018). A thoroughgoing design of a rapid-cycle microfluidic droplet-based PCR device to amplify rare DNA strands. *Journal of Applied Fluid Mechanics, 11*(1).

Oh, J. K., Drumright, R., Siegwart, D. J., & Matyjaszewski, K. (2008). The development of microgels/nanogels for drug delivery applications. *Progress in Polymer Science, 33*(4), 448–477.

Oraee-Yazdani, S., Hafizi, M., Atashi, A., Ashrafi, F., Seddighi, A., Hashemi, S., Seddighi, A., Soleimani, M., & Zali, A. (2016). Co-transplantation of autologous bone marrow mesenchymal stem cells and Schwann cells through cerebral spinal fluid for the treatment of patients with chronic spinal cord injury: Safety and possible outcome. *Spinal Cord, 54*(2), 102.

Park, H., Temenoff, J. S., Holland, T. A., Tabata, Y., & Mikos, A. G. (2005). Delivery of TGF-β1 and chondrocytes via injectable, biodegradable hydrogels for cartilage tissue engineering applications. *Biomaterials, 26*(34), 7095–7103.

Pittenger, M. F., Mackay, A. M., Beck, S. C., Jaiswal, R. K., Douglas, R., Mosca, J. D., Moorman, M. A., Simonetti, D. W., Craig, S., & Marshak, D. R. (1999). Multilineage potential of adult human mesenchymal stem cells. *Science, 284*(5411), 143–147.

Putney, S. D. (1998). Encapsulation of proteins for improved delivery. *Current Opinion in Chemical Biology, 2*(4), 548–552.

Rasouli, M., Mehrizi, A. A., Goharimanesh, M., Lashkaripour, A., & Bazaz, S. R. (2018). Multi-criteria optimization of curved and baffle-embedded micromixers for bio-applications. *Chemical Engineering and Processing-Process Intensification, 132*, 175–186.

Re'em, T., Kaminer-Israeli, Y., Ruvinov, E., & Cohen, S. (2012). Chondrogenesis of hMSC in affinity-bound TGF-beta scaffolds. *Biomaterials, 33*(3), 751–761.

Ren, K., Cui, H., Xu, Q., He, C., Li, G., & Chen, X. (2016). Injectable polypeptide hydrogels with tunable microenvironment for 3D spreading and chondrogenic differentiation of bone-marrow-Derived mesenchymal stem cells. *Biomacromolecules, 17*(12), 3862–3871.

Rhee, M., Valencia, P. M., Rodriguez, M. I., Langer, R., Farokhzad, O. C., & Karnik, R. (2011). Synthesis of size-tunable polymeric nanoparticles enabled by 3D hydrodynamic flow focusing in single-layer microchannels. *Advanced Materials, 23*(12), H79–H83.

Romero-Cano, M. S., & Vincent, B. (2002). Controlled release of 4-nitroanisole from poly (lactic acid) nanoparticles. *Journal of Controlled Release, 82*(1), 127–135.

Soleimani, S., Hasani-Sadrabadi, M. M., Majedi, F. S., Dashtimoghadam, E., Tondar, M., & Jacob, K. I. (2016). Understanding biophysical behaviours of microfluidic-synthesized nanoparticles at nano-biointerface. *Colloids and Surfaces B, Biointerfaces, 145*, 802–811.

Vardar, E., Larsson, H. M., Allazetta, S., Engelhardt, E. M., Pinnagoda, K., Vythilingam, G., Hubbell, J. A., Lutolf, M. P., & Frey, P. (2018). Microfluidic production of bioactive fibrin micro-beads embedded in crosslinked collagen used as an injectable bulking agent for urinary incontinence treatment. *Acta Biomaterialia, 67*, 156–166.

Wang, X., Wenk, E., Zhang, X., Meinel, L., Vunjak-Novakovic, G., & Kaplan, D. L. (2009). Growth factor gradients via microsphere delivery in biopolymer scaffolds for osteochondral tissue engineering. *Journal of Controlled Release, 134*(2), 81–90.

Yang, H. N., Choi, J. H., Park, J. S., Jeon, S. Y., Park, K. D., & Park, K.-H. (2014). Differentiation of endothelial progenitor cells into endothelial cells by heparin-modified supramolecular pluronic nanogels encapsulating bFGF and complexed with VEGF165 genes. *Biomaterials, 35*(16), 4716–4728.

Yazdani, S. O., Hafizi, M., Zali, A. R., Atashi, A., Ashrafi, F., Seddighi, A. S., et al. (2013). Safety and possible outcome assessment of autologous Schwann cell and bone marrow mesenchymal stromal cell co-transplantation for treatment of patients with chronic spinal cord injury. *Cytotherapy, 15*(7), 782–791.

Zhang, T., Wen, F., Wu, Y., Goh, G. S. H., Ge, Z., Tan, L. P., Hui, J. H. P., & Yang, Z. (2015). Cross-talk between TGF-beta/SMAD and integrin signaling pathways in regulating hypertrophy of mesenchymal stem cell chondrogenesis under deferral dynamic compression. *Biomaterials, 38*, 72–85.